REPORT DOCUMENTATION PAGE

Form Approved
OMB No. 0704-0188

1. AGENCY USE ONLY (Leave blank)	2. REPORT DATE	3. REPORT TYPE AND DATES COVERED
	31 Oct 01	Final

4. TITLE AND SUBTITLE

X-ray Computed Topography of Ultralightweight Metals

5. FUNDING NUMBERS

Grant No.
N00014-97-1-G021

6. AUTHOR(S)

John M. Winter, Jr. , and Robert E. Green. Jr.

7. PERFORMING ORGANIZATION NAME(S) AND ADDRESS(ES)

Center for Nondestructive Evaluation
Room 102, Maryland Hall, 3400 N. Charles St.
The Johns Hopkins University
Baltimore, MD., 21218-2681

8. PERFORMING ORGANIZATION REPORT NUMBER

NRL-31-Oct- 01

9. SPONSORING / MONITORING AGENCY NAME(S) AND ADDRESS(ES)

Naval Research Laboratory
NRL Code 3220-KM
4555 Overlook Ave SW
Washington, DC, 20375

10. SPONSORING / MONITORING AGENCY REPORT NUMBER

Not known

11. SUPPLEMENTARY NOTES

None

12a. DISTRIBUTION / AVAILABILITY STATEMENT

Unlimited Availability to the Public

13. ABSTRACT *(Maximum 200 words)*

In recent years, several universities, government laboratories, and private industries have been developing specific process technologies, analytical modeling tools, and characterization methods for highly porous metals and alloys frequently collectively termed "ultralightweight metals". The goal has been to achieve a family of metallic structures which are analogs to the organic cellular materials that exhibit high stiffness and a low specific weight. A number of quite different and distinct processes have evolved and are still largely not yet mature. To date, the imaging capabilities of x-ray computed tomography have not been generally employed to nondestructively examine the internal structure of the products formed by these various processes. This article briefly reviews the principles and terminology of x-ray computed tomography as it has evolved through successive generations and then presents several types of computed tomographic images of ultralightweight metallic specimens produced by different process technologies. The images for each specimen are preceded by a brief description of the process technology which created it.

14. SUBJECT TERMS	15. NUMBER OF PAGES
X-ray CT, Foam Metals, Porous Metals, Ultralightweight Metals Ultralight Metals, Microfocus X-ray Computed Tomography	29
	16. PRICE CODE

17. SECURITY CLASSIFICATION OF REPORT	18. SECURITY CLASSIFICATION OF THIS PAGE	19. SECURITY CLASSIFICATION OF ABSTRACT	20. LIMITATION OF ABSTRACT
Unclassified	Unclassified	Unclassified	Unlimited

GENERAL INSTRUCTIONS FOR COMPLETING SF 298

The Report Documentation Page (RDP) is used in announcing and cataloging reports. It is important that this information be consistent with the rest of the report, particularly the cover and title page. Instructions for filling in each block of the form follow. It is important to *stay within the lines* to meet *optical scanning requirements*.

Block 1. Agency Use Only *(Leave blank)*.

Block 2. Report Date. Full publication date including day, month, and year, if available (e.g. 1 Jan 88). Must cite at least the year.

Block 3. Type of Report and Dates Covered. State whether report is interim, final, etc. If applicable, enter inclusive report dates (e.g. 10 Jun 87 - 30 Jun 88).

Block 4. Title and Subtitle. A title is taken from the part of the report that provides the most meaningful and complete information. When a report is prepared in more than one volume, repeat the primary title, add volume number, and include subtitle for the specific volume. On classified documents enter the title classification in parentheses.

Block 5. Funding Numbers. To include contract and grant numbers; may include program element number(s), project number(s), task number(s), and work unit number(s). Use the following labels:

C	- Contract	PR	- Project
G	- Grant	TA	- Task
PE	- Program Element	WU	- Work Unit Accession No.

Block 6. Author(s). Name(s) of person(s) responsible for writing the report, performing the research, or credited with the content of the report. If editor or compiler, this should follow the name(s).

Block 7. Performing Organization Name(s) and Address(es). Self-explanatory.

Block 8. Performing Organization Report Number. Enter the unique alphanumeric report number(s) assigned by the organization performing the report.

Block 9. Sponsoring/Monitoring Agency Name(s) and Address(es). Self-explanatory.

Block 10. Sponsoring/Monitoring Agency Report Number. *(If known)*

Block 11. Supplementary Notes. Enter information not included elsewhere such as: Prepared in cooperation with...; Trans. of...; To be published in.... When a report is revised, include a statement whether the new report supersedes or supplements the older report.

Block 12a. Distribution/Availability Statement. Denotes public availability or limitations. Cite any availability to the public. Enter additional limitations or special markings in all capitals (e.g. NOFORN, REL, ITAR).

DOD	- See DoDD 5230.24, "Distribution Statements on Technical Documents."
DOE	- See authorities.
NASA	- See Handbook NHB 2200.2.
NTIS	- Leave blank.

Block 12b. Distribution Code.

DOD	- Leave blank.
DOE	- Enter DOE distribution categories from the Standard Distribution for Unclassified Scientific and Technical Reports.
NASA	- Leave blank.
NTIS	- Leave blank.

Block 13. Abstract. Include a brief *(Maximum 200 words)* factual summary of the most significant information contained in the report.

Block 14. Subject Terms. Keywords or phrases identifying major subjects in the report.

Block 15. Number of Pages. Enter the total number of pages.

Block 16. Price Code. Enter appropriate price code *(NTIS only)*.

Blocks 17. - 19. Security Classifications. Self-explanatory. Enter U.S. Security Classification in accordance with U.S. Security Regulations (i.e., UNCLASSIFIED). If form contains classified information, stamp classification on the top and bottom of the page.

Block 20. Limitation of Abstract. This block must be completed to assign a limitation to the abstract. Enter either UL (unlimited) or SAR (same as report). An entry in this block is necessary if the abstract is to be limited. If blank, the abstract is assumed to be unlimited.

X-ray Computed Tomography of Ultralightweight Metals

John M. Winter, Jr.[#], and Robert E. Green, Jr.[*],

[#]Principal Research Scientist, Center for Nondestructive Evaluation
[*]Principal Research Scientist & Former Director of the Center for Nondestructive Evaluation
and
Professor, Department of Materials Science and Engineering

The Johns Hopkins University, Baltimore, MD., 21218-2608

FINAL REPORT

Grant No. N00014-97-1-G021
Naval Research Laboratory
4555 Overlook Ave, SW
Washington, DC, 20375-5320

October 31, 2001

ABSTRACT

In recent years, several universities, government laboratories, and private industries have been developing specific process technologies, analytical modeling tools, and characterization methods for highly porous metals and alloys frequently collectively termed "ultralightweight metals". The goal has been to achieve a family of metallic structures which are analogs to the organic cellular materials that exhibit high stiffness and a low specific weight. A number of quite different and distinct processes have evolved and are still largely not yet mature. To date, the imaging capabilities of x-ray computed tomography have not been generally employed to nondestructively examine the internal structure of the products formed by these various processes. This report briefly reviews the principles and terminology of x-ray computed tomography as it has evolved through successive generations, and presents computed tomographic images in several formats of many types of ultralightweight metallic specimens which have been produced by a variety of organizations using different process technologies. The images for each specimen are preceded by a brief description of the process technology which created it. In conclusion, a brief summary of the authors interactions with others in the ultralightweight community is given..

Introduction

Highly porous materials are known to have a high stiffness combined with a very low specific weight. Such cellular materials frequently occur in nature as organic structural materials, (e.g. wood and bones). The fact that metals and alloys can be produced as cellular solids or metal foams is not as widely known [1]. This emerging technology produces metals and alloys which have been fabricated with intentional porosity or voids to achieve reduced weight with minimum sacrifice in strength. Recently, computed tomography, (CT), has been used by the authors of this report to nondestructively image the internal structure of such ultralightweight metallic materials produced by several of these evolving processes. Since computed x-ray tomography is quite different from the more familar x-ray radiography, it is appropriate to examine the difference between the two.

X-ray radiography and its most recent form, "Digital Radiography"

X-ray radiography generates an image which is essentially a transmission shadowgram. The shades of gray represent differences in absorption imposed on the transmitted rays which follow different paths through the object under study. Except for objects with very simple internal structure, interpretation of the locations, shapes, sizes, and densities of absorbers cannot be unique, because the single view in transmission does not distinguish between single absorbers and multiple absorbers overlapping the same ray paths. Historically, radiography has used film as an image detector (e.g. for chest x-rays). More recently an electronic alternative, "Digitital Radiography" or "DR" has come into use. Image data is collected by pixels which are readily digitized for subsequent computer-based image processing and/or archiving. The detectors for DR generally use either a "Linear Detector Array" (LDA) which is a linear array of phototransistors or an image intensifier combined with a CCD (charge coupled device) camera or a CID (charge injection device) camera. In both cases some type of phosphor is used to convert the x-ray photons to visible photons to enchance the image signal strength for the detectors. Either the LDA or the camera system provide analog pixel-by-pixel outputs which are then digitized (typically with 12 bit or better resolution) and processed by computer. Figure 1 shows the geometry for producing a DR of a testpiece using a LDA detector. In this example, the LDA and an x-ray source with a divergent thin horizontal fan beam of x-rays both lie in a plane, and the testpiece is translated along a direction perpendicular to that plane. The LDA collects, digitizes, and stores x-ray intensity data continuously as the testpiece moves through the beam, allowing the assembly of a complete radiograph when the vertical scan is completed.

Principles of computed x-ray tomography, [2, 3]

In the example just shown in Fig 1, if the testpiece were kept stationary instead of translating vertically through the x-ray beam, the line of radiographic image data collected by the LDA in the plane of the divergent thin horizontal fan beam would be termed a "view". Tomography is based on collecting a multitude of radiographic views from different directions. For example, one particular configuration for tomography would use the same geometry shown in Figure 1, except instead of translating the testpiece vertically to generate a DR, the testpiece would be rotated about its own vertical axis to allow the

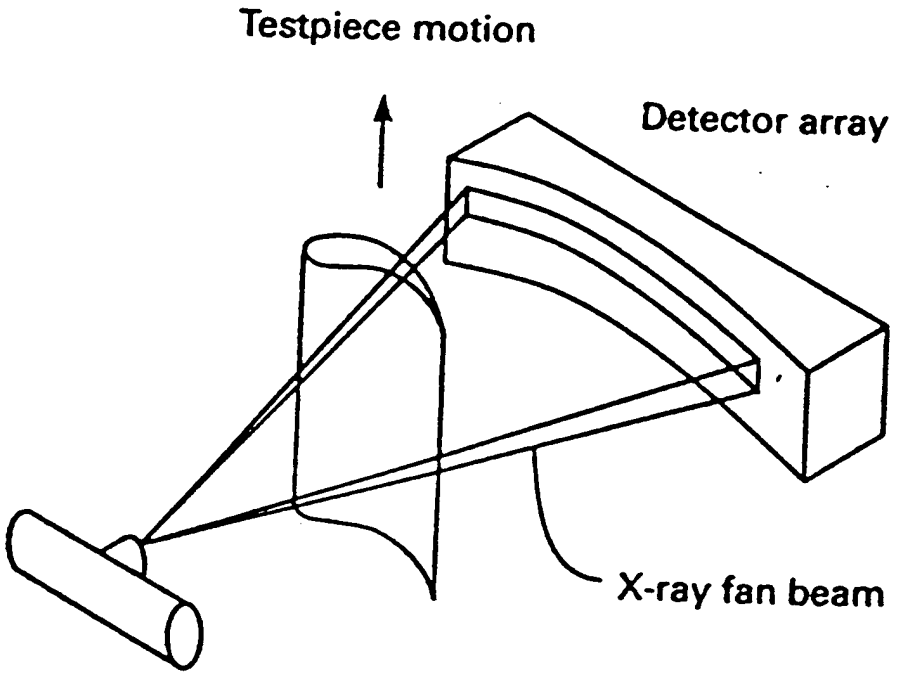

Figure 1. Arrangement for producing a digital radiograph, (DR), using a linear detector array, (LDA)

LDA to generate a whole set of different views from different directions in the same plane. Typically 1500 views might be generated in the course of a 360^0 rotation. Each of these views has its own unique distribution of x-ray intensities along the line of LDA pixels. With the proper computer algorithm, a unique 2-dimensional image can be generated from these views which will show the locations, shapes, sizes, and densities of absorbers which are in the only possible arrangement which could give rise to the intensity data recorded in the entire set of views. This 2-dimensional image computed from the set of views is termed a "slice" One might then translate the testpiece incrementally along its vertical axis, and collect another set of 1500 views. Repeating this process to collect a whole set of contiguous 2-dimensional slices allows the computer to construct a 3-dimensional volume showing the complete internal structure of the testpiece. The resulting volume is termed a "Multiple Plane Reconstruction" (MPR). Computer software facilitates displaying images on any plane cutting through the MPR at any location and at any angle, independent of the orientation of the original family of contiguous slices used to construct the MPR. Another feature typical of available software allows construction of a MPR of a selected set of slices to create a 3-dimensional volume which can be rotated in space to allow viewing from any direction under illumination from a computer generated light source which can shadow surface irregularities from any arbitrary direction. This feature is termed a "volume rendering".

The evolution of computed tomographic generations

Historically, much of the evolution of computed tomography was driven by medical applications. In medical CT systems, the x-ray source and detector are generally rotated or translated so that the patient may remain stationary. In industrial systems, the mechanics of the geometry can usually be greatly simplified by rotating or translating the component under study instead. The evolution of CT geometries has gone through four basically different methods, or generations. The first generation used a collimated pencil beam x-ray source with a single point detector. The industrial version of the first generation let the object under study translate in a horizontal direction across the pencil beam while the point detector collected data. The object would then be rotated a small increment about a vertical axis, and the translation repeated. The process was repeated until a complete rotation was achieved, and a 2-dimensional slice could be constructed. This was the original so-called "translate-rotate" system. The second generation geometry was also a translate-rotate system, but the pencil beam source was replaced with a divergent thin horizontal fan beam and a linear array of coarsely spaced multiple detectors. The object was translated along an axis lying in the plane of the fan beam, incrementally rotated, and translated again, in the same fashion as used in the first generation. The advantage of this arrangement was that more individual rays of x-rays and more detectors were involved at any instant in time, allowing data collection to proceed faster. The third generation, known as a rotate-rotate system, used many closely spaced detector elements (a LDA) and a divergent thin horizontal fan beam similar to that used in the second generation. The nomenclature refers to the medical version wherein the patient was stationary and both the x-ray source and the LDA would rotate synchronously around the patient in a plane. In the industrial version, the object under study was rotated instead,

while the x-ray source and the LDA remain fixed. Unlike generations one and two, no translation was involved. Hence it became known as a "rotate only" configuration. A fourth generation geometry exists for medical applications wherein a stationary LDA detector ring completely surrounds the patient, and only the x-ray source rotates around the patient on a ring of smaller diameter than the detector ring and in the same plane as the detector ring. This configuration has become known as the "stationary detector-rotate only" arrangement. As far as we know, the fourth generation version has no industrial analogs.

Methods for preparing ultralightweight metals and the resulting structures

A variety of methods for forming open or closed cell foams in alloys ranging from aluminum alloys to copper, titanium, and steel have been demonstrated by various investigators. Depending on the particular process employed, porosities may range from about 5 percent all the way up to 95 percent. Each of the following sections briefly describe the highlights of selected processes along with some representative internal structures as revealed by x-ray computed tomography.

The Gasar Process [4]

The key step in the Gasar process is to saturate a melt contained in a high pressure furnace with hydrogen from a high pressure mix of hydrogen and argon, (e.g. 10 to 50 atmospheres). Then the furnace is quickly depressurized to one atmosphere, the melt is poured into a mold, and subsequently the molten casting is directionally solidified from bottom to top as rapidly as possible. Dissolved gas rejected from the solid during solidification forms bubbles at the liquid-solid interface during solidification and these bubbles tend to grow to form long tubular voids as the interface progresses upward.

Illustrative details of the image collection process for a Gasar specimen

CT data was collected using a 25mm diameter cylinder of aluminum produced in the Ukraine by the Gasar process. The CT method employed was third generation with a centered table. The x-ray source was a Kevex microfocus tube operating at 160 Kev and 0.050 mA, with a 20 micron focal spot size. The detector was an image intensifier combined with a CCD camera. The source-to-(image) detector distance (SID) was 648 mm. The source-to-object distance (SOD) was 45 mm. The nominal magnification as given by SID/SOD was 14X.

The data collection geometry was the following:

Number of rays per view 512
Number of views per slice (all the views in the same plane) 1800
Height (or thickness) per slice 0.10 mm
Number of slices taken 50
Total height of the volume reconstruction 5 mm
Field of reconstruction (the diameter of the sampled volume) 12mm
Dynamic range of each detector pixel 12bits (4096 shades of gray)

CT images of the Gasar specimen

Figure 2 shows the reconstructed image of a 12mm diameter circular slice 0.1 mm thick excised from the middle of the 25 mm diameter cylindrical specimen. In this image, (as in all the subsequent images), white represents an absorber of x-rays, and black represents voids. The plane of the CT slice was perpendicular to the axis of the cylinder and located about half way up the height of the cylinder.. The image was reconstructed from 1800 views acquired from different directions as the specimen was rotated in a third generation (rotate only) geometry.

Figure 3 shows a multiple plane reconstruction (MPR) from a full set of 50 CT slices. The circular image in Fig.3 is just a smaller version of Fig. 2. The rectangular images located below and located to the right of the circular image in Fig. 3 are images of reconstructed internal slices looking along radial directions perpendicular to the cylinder axis. They are the result of a multiple plane reconstruction of the 50 contiguous slices, each 0.1 mm thick. The "short" dimension of the rectangular images is merely the height of the 50 reconstructed slices, or 5 mm. The "long" dimension of a rectangular image corresponds to the diameter where the plane of the rectangular image slices the circular cross-section. Dashed diametral lines in the circular image show the locations of the top edges of the surfaces being viewed. The fourth image in Fig. 3 is a view of a surface passing from top to bottom of the 12 mm diameter cylinder, but tilted with respect to the cylinder axis. The long edge starts on the top surface at the diameter. The short edge corresponds to the length of the chord defined where the reconstrucyted plane cuts through the bottom surface. The combination of these three different views provide convincing evidence that the porosity is in the form of tubes which run parallel to the growth direction. This observation supports the prediction of the solidification model for the process.

The Georgia Tech Hollow Sphere Process [5].

This is a technology, (under development at Georgia Tech), that forms uniform, thin-walled hollow spheres as separate entities which may then subsequently be bonded at points of contacts into foams, [5]. Monosized thin-walled spherical shells are formed when slurries containing constituent powders and polymer dispersants are injected through the outer jet of a coaxial nozzle. Gas passing through the inner jet of the nozzle forms bubbles. Slurry exits the nozzle in the form of a hollow cylinder that pinches off, (due to surface tension and hydrostatic forces), forming a hollow sphere. The sphere hardens in free flight as solvent evaporates, and subsequently undergoes a sintering operation. The process forms spheres at rates of 3,000 to 15,000 spheres/min with typical production rates of 2 to 7 kg/hr from a single nozzle.

Figure 4 is an example of a digital radiograph, or "DR", as discussed previously (p.3). In this case it is a single "view" of the side of a cylinder fabricated at Georgia Tech from their hollow steel balls which have been fused together into a monolithic assembly.

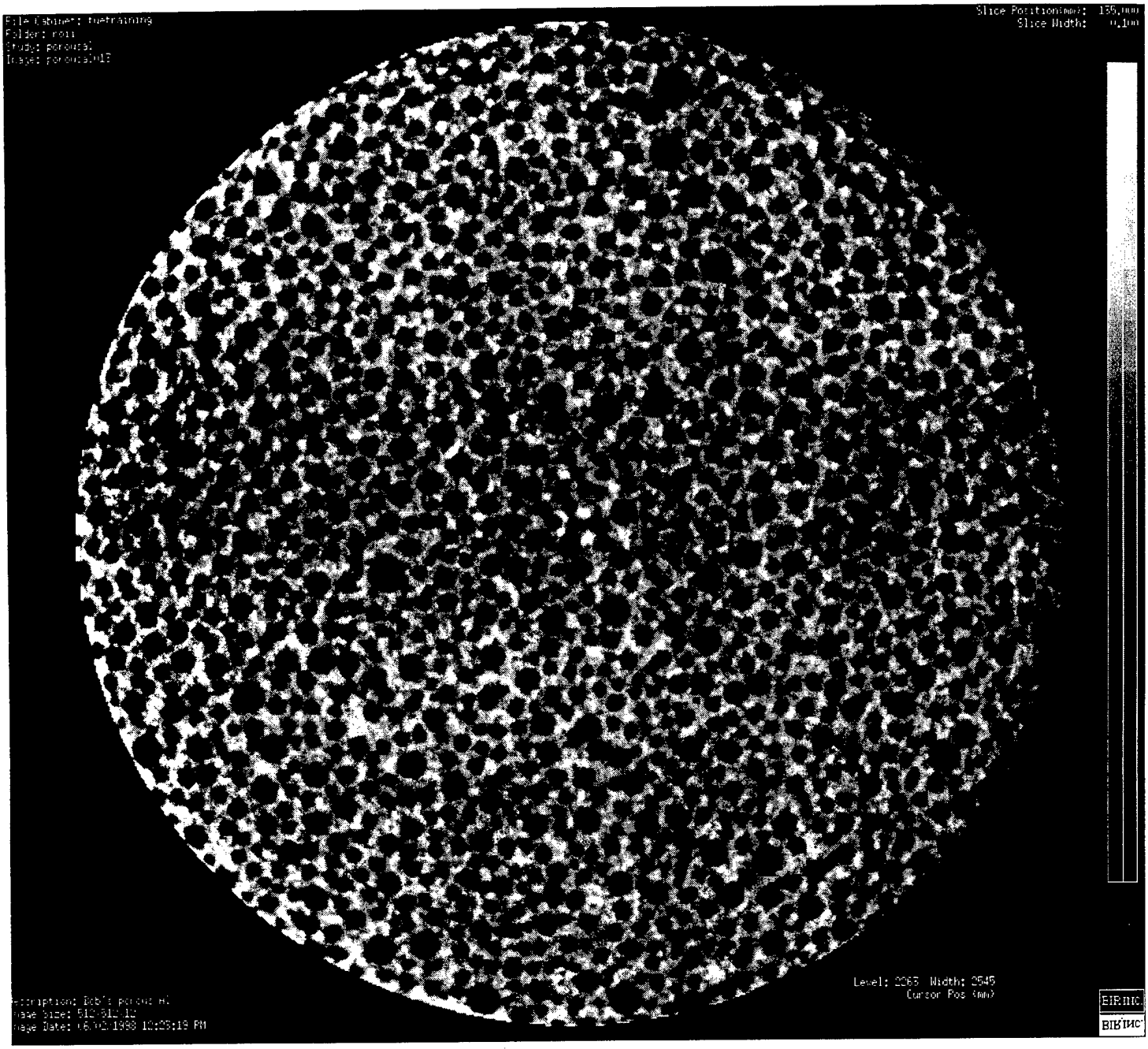

Figure 2. Reconstructed image of a circular slice excised from the middle of the 25 mm diameter cylindrical specimen fabricated using the Gasar process

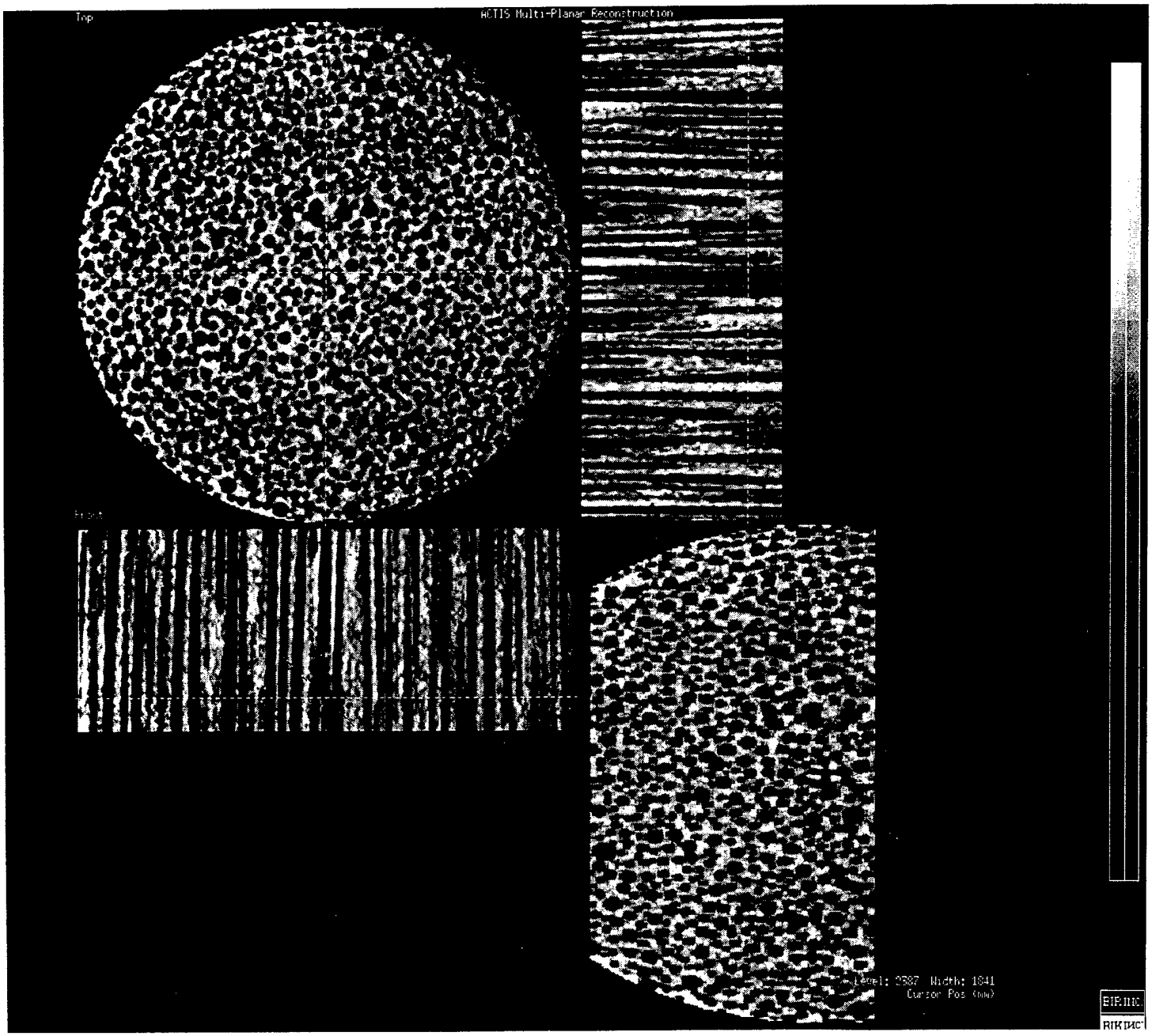

Figure 3. Multiple plane reconstruction, (MPR), images captured from a cylinder of aluminum fabricated by the Gasar process to create tubular porosity

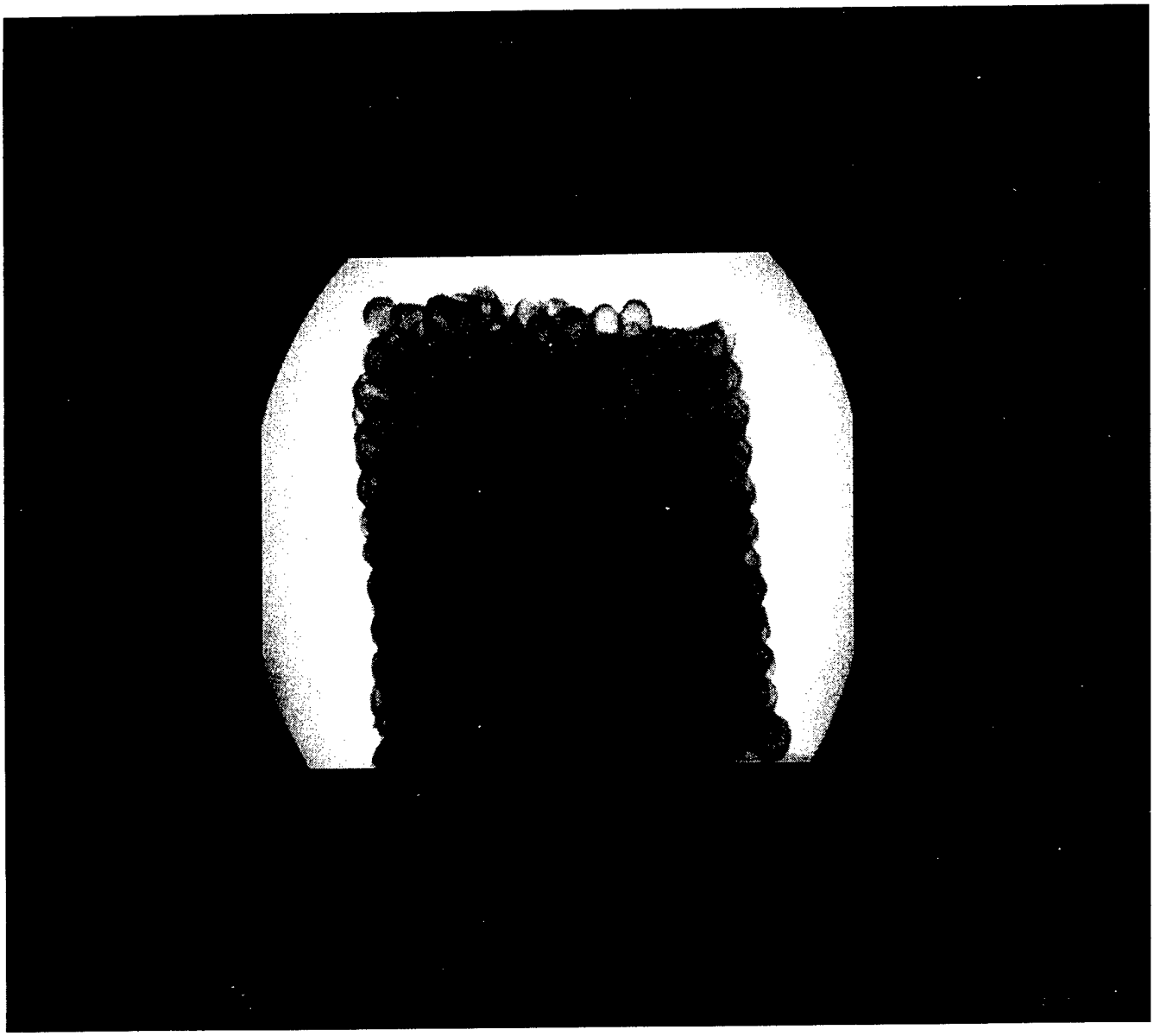

Figure 4. Digital radiograph, (DR), showing a single "view" of the side of a cylinder fabricated at Georgia Tech from their hollow steel balls

Figure 5 shows a multiple plane reconstruction, (MPR), of a monolithic assembly of hollow steel spheres which form a right circular cylinder 23 mm in diameter and 20 mm high. The data was generated with 160 keV x-rays with 0.05 mA beam current focussed into a 20 micron spot on the x-ray tube anode. The circular image in Fig. 5 is the reconstruction of an internal plane encompassing the entire 23 mm cross-section. As with Fig. 3, the two rectangular images are reconstructions of the images on planes orthogonal to radial directions which would be revealed by cutting away sides of the cylinder. And, as in Fig. 3, the fourth image is a cut-away view on an internal plane which is tilted with respect to the axis of the cylinder. The straight edges of this latter view are chords on the top and bottom surfaces, respectively, of the cylindrical specimen. The bowed (curved) edges are traces delineating the intersection of the edges of the surface of the cylindrical specimen with the tilted plane of the image.

Figure 6 shows a CT slice which was taken from the same specimen as the one which was examined in Fig. 5, except that only a part of the entire 23 mm diameter cylinder was scanned. The scanned field in Fig. 6 was an 8.9 mm diameter slice of the central portion of the total cylinder. The slice was reconstructed from 2000 in-plane views. Details of the bonding between spheres and wall thickness are better resolved in this image than in Fig. 5 because of the higher magnification. Off-line image processing measurement tools permit accurate measurement of virtually any selected feature in the image. The locations of dimensional measurements on this image can be seen where the short intensified white lines are shown. Such a line can be seen on the wall of the hollow ball located on the perimeter of the slice at about 2 o'clock. On close examination, the faint white number "1" can be seen in the hollow of the sphere not far from the line. At the top left of the figure, measurement data for the wall thickness under line 1 is listed. Further close examination of this data list shows the wall thickness for line 1 is "0.0897072" mm. A more reasonable value could be taken as 0.090 mm. A subjective observation is that as little as one-third of the wall thickness could be considered as a reasonable minimum feature size which could be resolved visually. This would correspond to a resolution of features as small as 30 microns.

Figure 7 is a slice taken from a specimen again fabricated at Georgia Tech, but reflecting the technology about a year earlier than the sample examined in the previous figures. This specimen is an elliptical cylinder, with a 35mm x 45mm oval cross-section and 33mm high. The linear flaws in the uniform packing shown in Fig. 7 are reminescient of those shown by the classic materials science demonstration of the dynamic motion of dislocations illustrated by the famous Bragg Bubble Raft. Figure 8 shows a volume rendering of a the multiple plane reconstruction which used slices including the one shown in Fig. 7. In such a rendering, the reconstruction may be rotated so as to be viewed from any arbitrary angle and illuminated with an imaginary lamp from any arbitrary direction. Note the packing flaws again shown in the surface. Finally, Fig. 9 shows a slice of the same specimen which was generated at LLNL using their unique "LCAT" system.

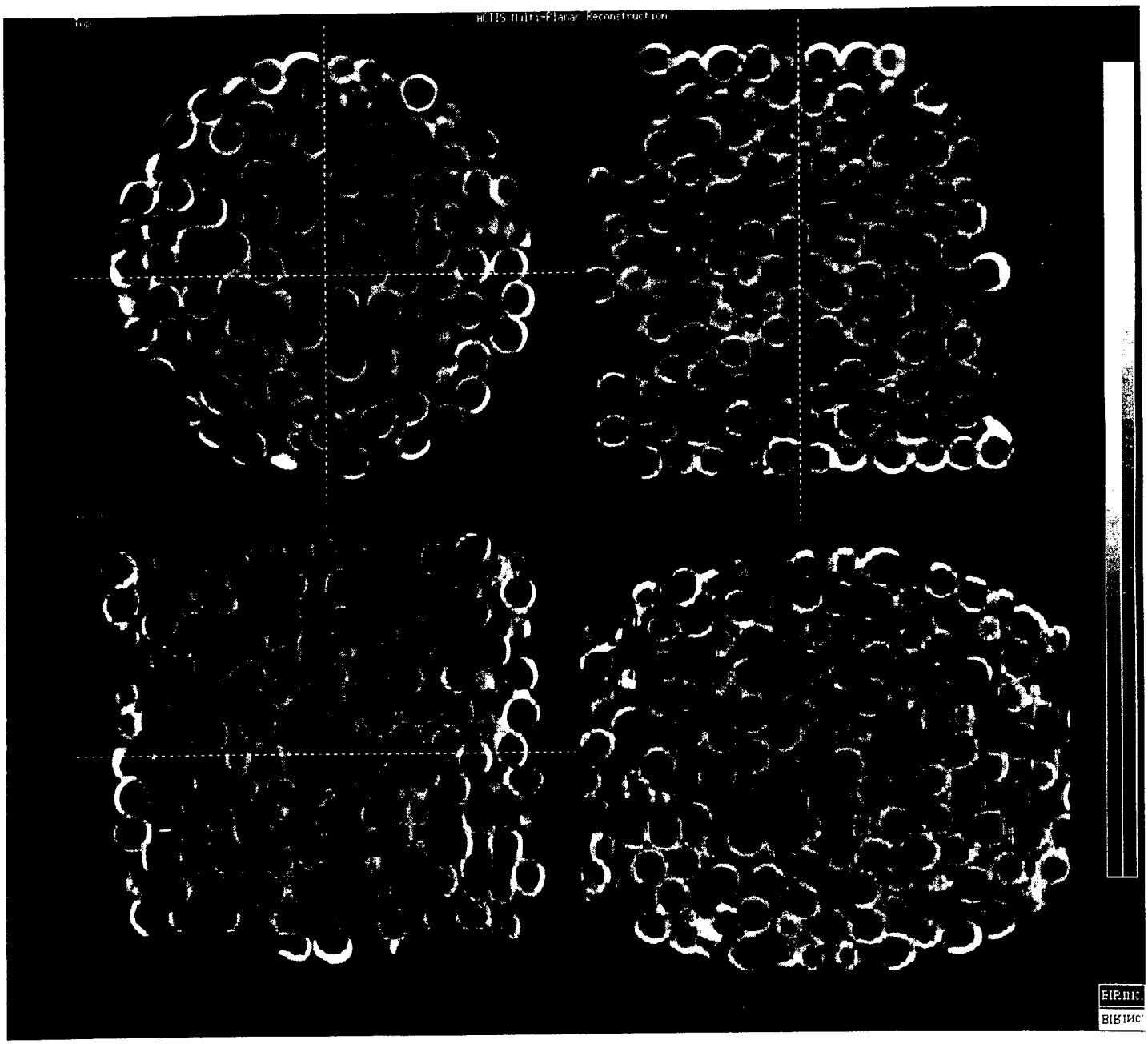

Figure 5. A multiple plane reconstruction, (MPR), of a monolithic assembly of hollow steel spheres using a process developed at Georgia Tech

Figure 6. An 8.0 mm diameter central portion of the same 23 mm diameter cylinder as shown in Fig. 5, except this data set was collected by re-scanning with a narrower fan beam

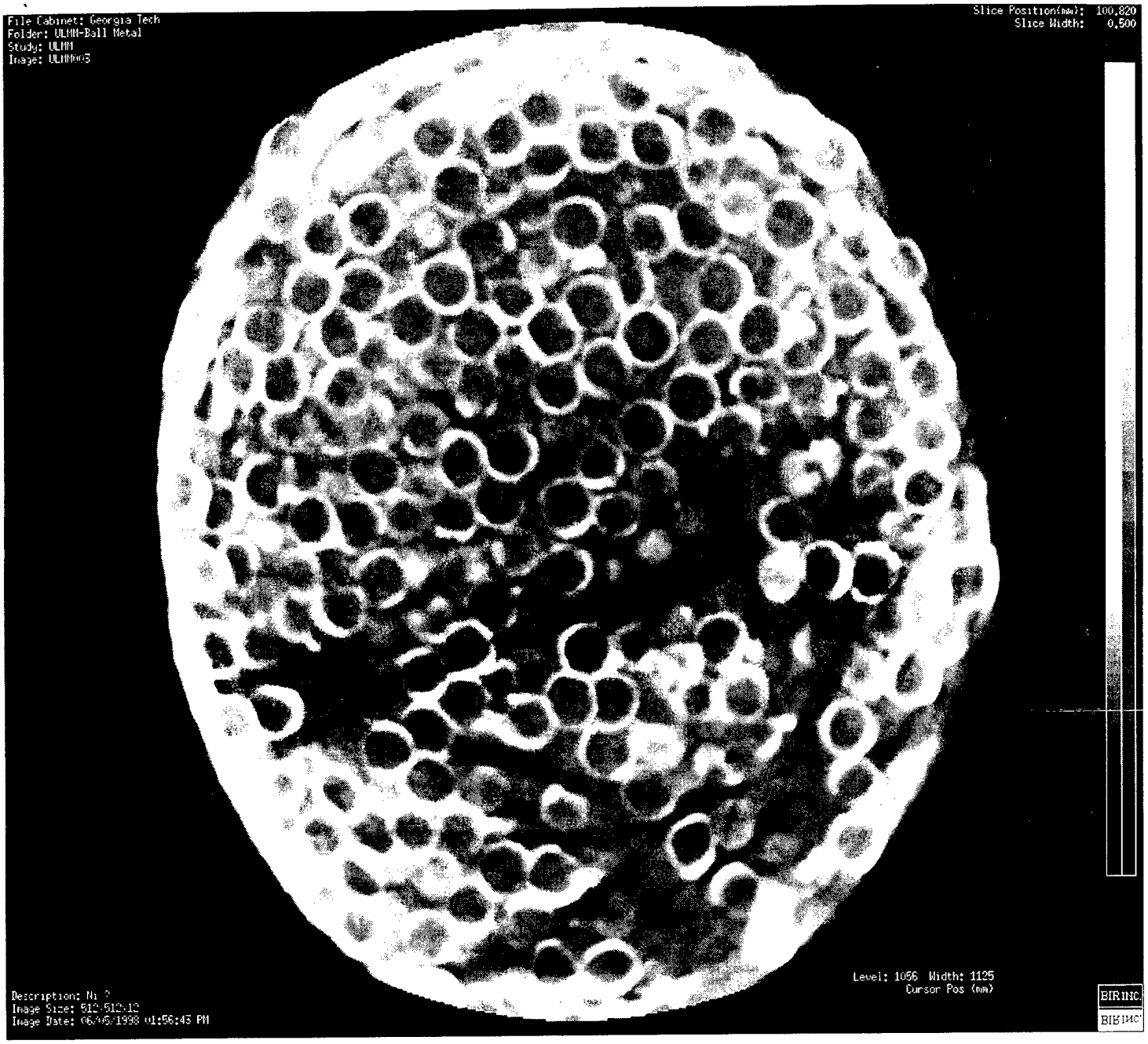

Figure 7. CT slice from another specimen fabricated at Georgia Tech, but reflecting the technology about a year earlier than the specimen shown in Fig. 6

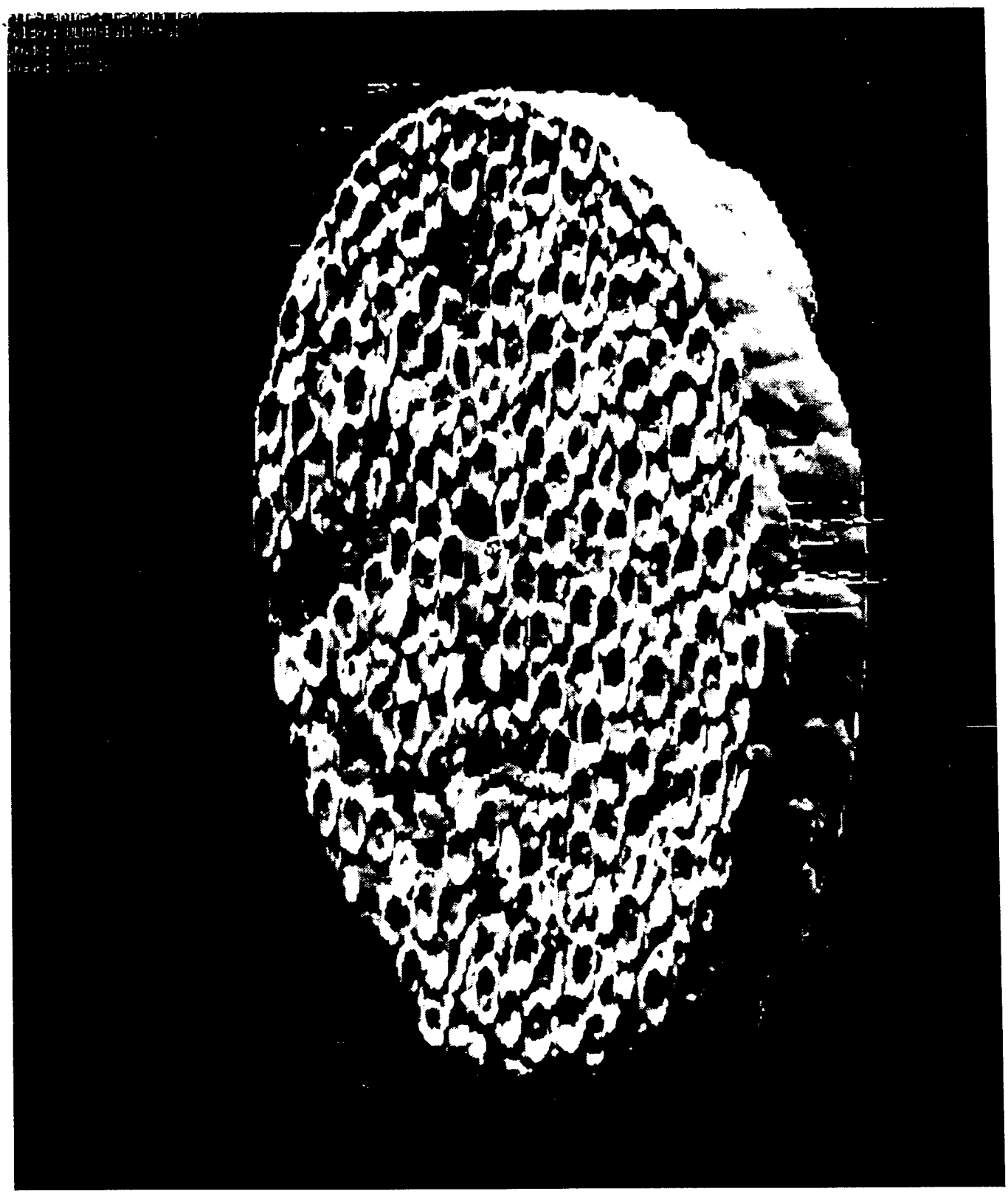

Figure 8. Volume rendering of the MPR of the specimen shown in Fig. 7

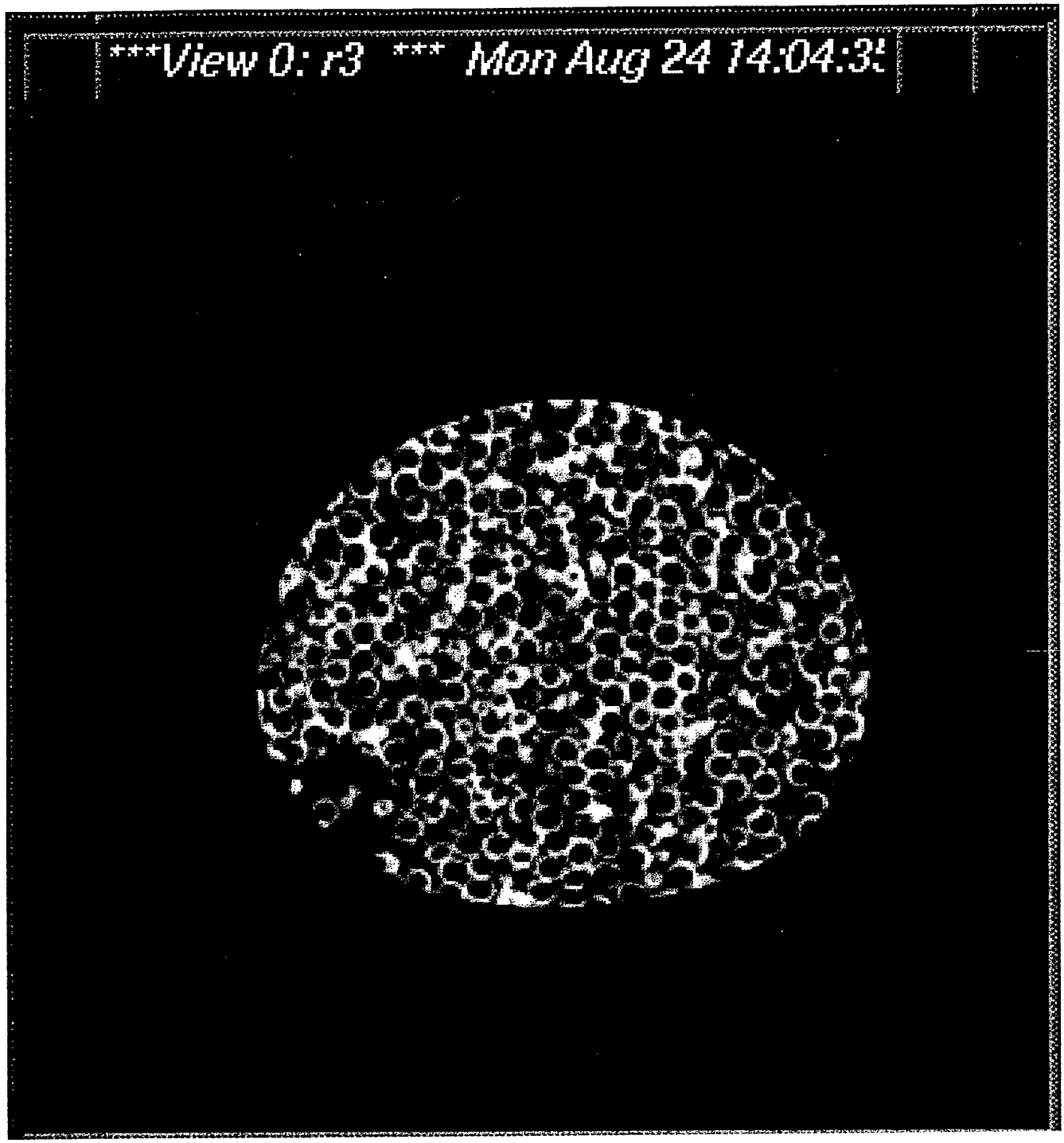

Figure 9. CT slice of same specimen as shown in Figs. 7 and 8, only this image was acquired with the LCAT system at LLNL

The Alporas Process [6]

Another process for generating ultralightweight metals is the Alporas process for generating foam aluminum material. In this technology, adding calcium to the aluminum alloy melt increases its viscosity (probably by forming an aluminum-calcium intermetallic). A discrete foaming agent is added to the melt. The foaming agent decomposes under the influence of heat and releases gas which drives the foaming process. This process has been developed and commercialized by the Shinko Wire Co., Ltd in Amagasaki, Japan. Their process involves increasing the viscosity of the melt to inhibit the rate of bubble flotation by adding about 1.5% Ca to the melt. The melt is then poured into a casting mold and stirred with an admixture of 1.6% titanium hydride as a foaming agent. The specimen was fabricated at United Technologies Research Center.
Again, the data was acquired using the LLNL "LCAT" system. This particular data set was taken at 160 KeV tube voltage and 1.9 mA tube current, recording 17 slices 0.5 mm thick with each slice formed from 360 views. Magnification of the parent plate was 1.1 based on the SID/SOD ratio. Figure 10 shows a CT slice of the entire central plane of the specimen which was 64 mm square. The foam interior was 5 mm thick with additional solid face plates 1 mm thick bonded to each face, for a total thickness of 7 mm. This slice was acquired with 360 views per slice.

The Cymat Process

A method for directly foaming melts of aluminum alloys is being developed both by Cymat (originally by Alcan) in Canada, and subsequently Norsk Hydro, in Norway [1]. The process involves using additives such as silicon carbide, aluminum oxide, or magnesium oxide particles to enhance the viscosity of the aluminum melt. The melt is then foamed by blowing gases such as air, nitrogen, or argon into it using specialized rotating impellers to produce very fine gas bubbles and to distribute them homogeneously. Foaming agents are not used. The foam produced this way floats to the surface of the melt and can be pulled off (by a conveyer belt) as the product. Figure 11 shows a CT slice of a foamed aluminum slab produced by the Cymat process. The scale is given by noting the image encompasses the entire slab which is 152 mm square and 51 mm thick. Note the large variations in the size of the porosity. In general, modeling efforts on foamed metal structures show that the best mechanical properties can be expected from the processes which produce the most uniform porosity size and distribution.

The Low Density Core Process

The low density core (LDC) process which is yet another process practiced in the field of ultralight porous materials [4,5]. It is an entirely different approach. Processing starts with metal powders instead of molten metals. One method has been invented and patented by the Fraunhofer Institute for Applied Materials Research, (IFAM), in Bremen, Germany. Powder of the desired alloy is packed into a canister, which is outgassed and then charged with 300 to 500 kPa (absolute) of Ar gas. The canister is sealed and hot isostatically pressed (HIPed) under carefully selected temperature and pressure conditions. The entrapped gas is highly compressed into a volume hundreds of time less than it initially occupied. The typical porosity at this stage is about 2%. The canister is then hot worked (rolling, pressing, or extrusion) tnto a near net final shape. The part is

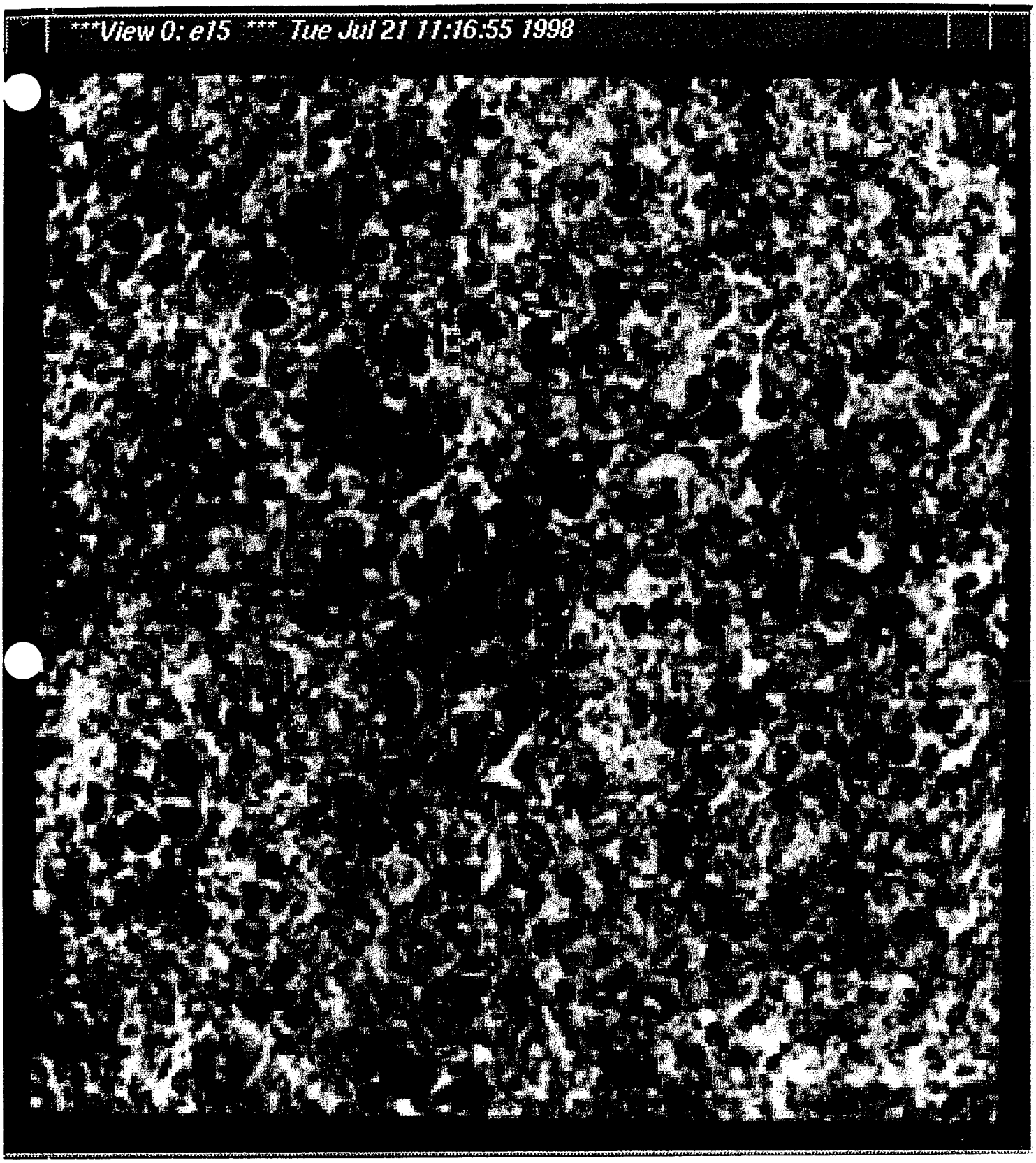

Figure 10 A 2-dimensional CT slice of a central plane extending edge-to-edge in a 64 mm square plate made by the Alporas process

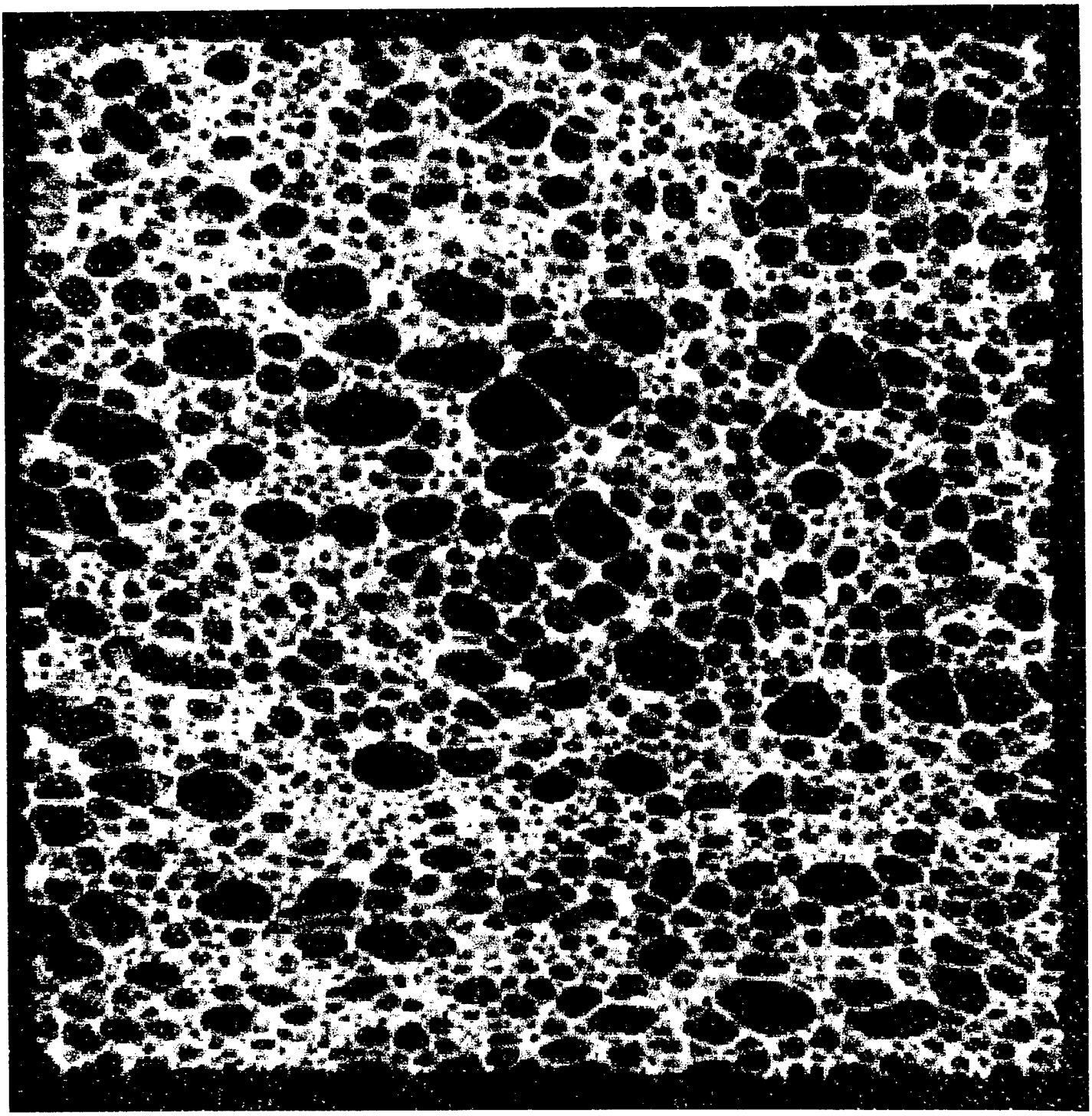

Figure 11. A 2-dimensional CT slice of a foamed aluminum slab produced by the Cymat process. The image encompasses the entire 152 mm square slab.

subjected to a final expansion annealing treatment to obtain a part with 20 to 40% of largely unconnected pores. The walls of the original cannister serve as solid face sheets covering the porous inner core material of the final product. Figure12 shows a slice of an aluminum LDC plate produced by LKR in Austria using this procedure. This CT slice was again obtained using the LLNL "LCAT" system.

A different example of the LDC process was provided by the Fraunhofer USA Resource Center in Newark, Delaware. It was made of 6061 aluminum alloy, with a measured final porosity of 62%. In this case, the mixed powder with its foaming agent was compacted and heated in a closed copper die [7]. The CT slice shown in Fig. 13 goes from edge to edge of the 100 mm square specimen, and it displays the internal structure of a plane near the center of the 6.4 mm thick plate. This 2-dimensional CT slice was acquired with a 160 kV source voltage, 50 mA beam current, and a 20 micron spot size. Slice thickness was 0.1 mm, and 2400 views were acquired as the specimen rotated in the fan beam. Subsequent experiments showed the white artifacts were the result of the procedure used to load the mixed powder, and the artifacts did not appear after modifying the procedure for loading. Figure 14 is a volume rendering of a portion of the MPR used to get Figure 13.

A third example of the LDC process was a first effort to make "foamed steel" by UltraClad Corporation in Andover, MA. Figure 15 shows a digital radiograph of a cylinder excised from the foamed steel panel. The slab at the top is a circular piece of the face plate which came out as part of the excised cylinder. Figure 16 shows a central slice perpendicular to the cylinder axis, and two cuts, each perpendicular to diameters of the cylinder which themselves are orthogonal to each other. The final view is a plane tilted with respect to the axis of the cylinder in the same fashion as shown in previous examples. Each slice is reconstructed from 3000 in-plane views. Each slice covers the full diameter of the specimen, which is 20 mm. Each slice is 0.25 mm thick.

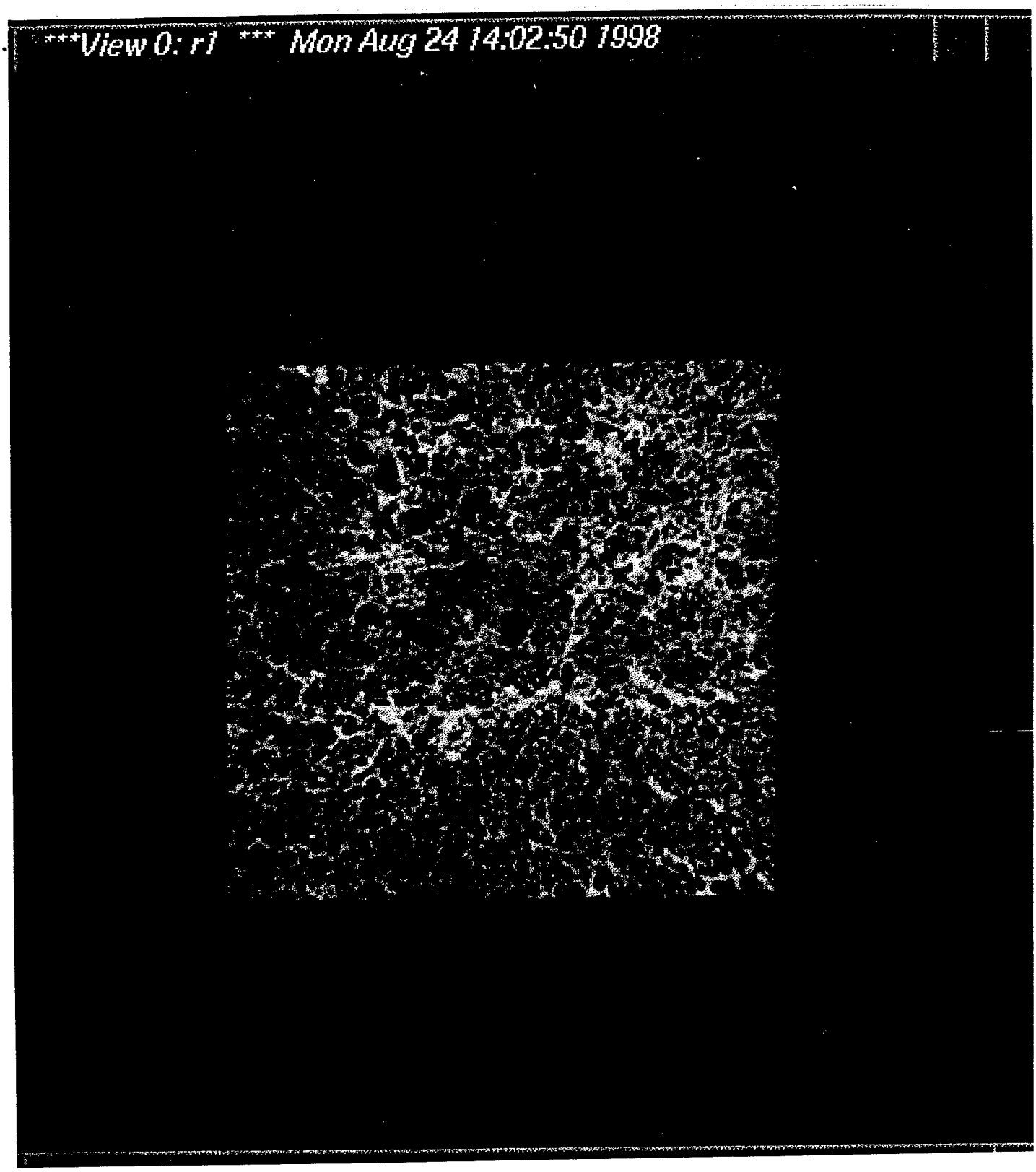

Figure 12. CT slice of an aluminum LDC (Low Density Core) plate produced by LKR in Austria using the powder metallurgy process developed by the Fraunhofer Institute

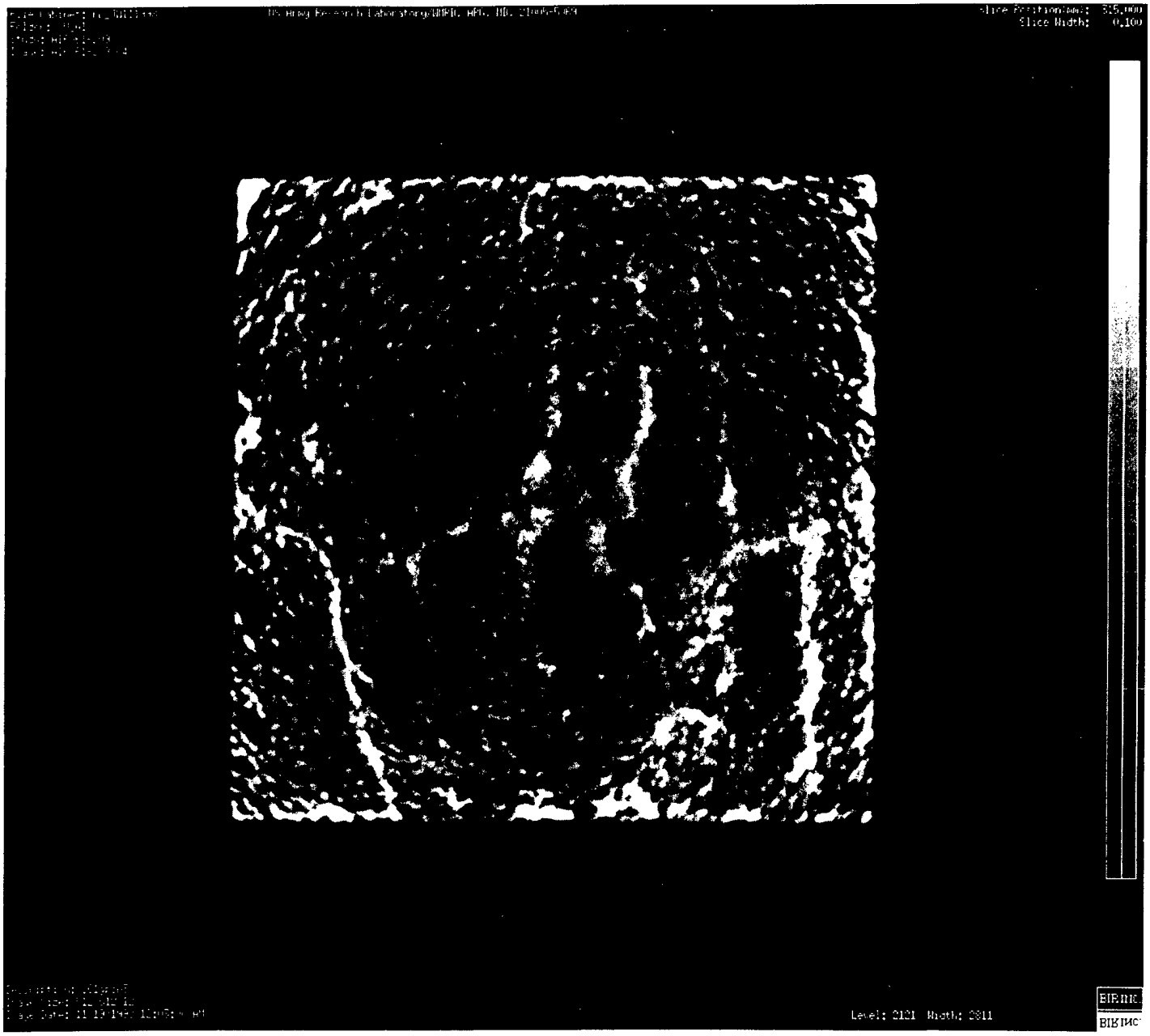

Figure 13. This CT slice extends from edge to edge on a central plane within a 100 mm square porous aluminum slab produced in a version of the LDC (Low Density Core) process used by Fraunhofer in Newark, Delaware

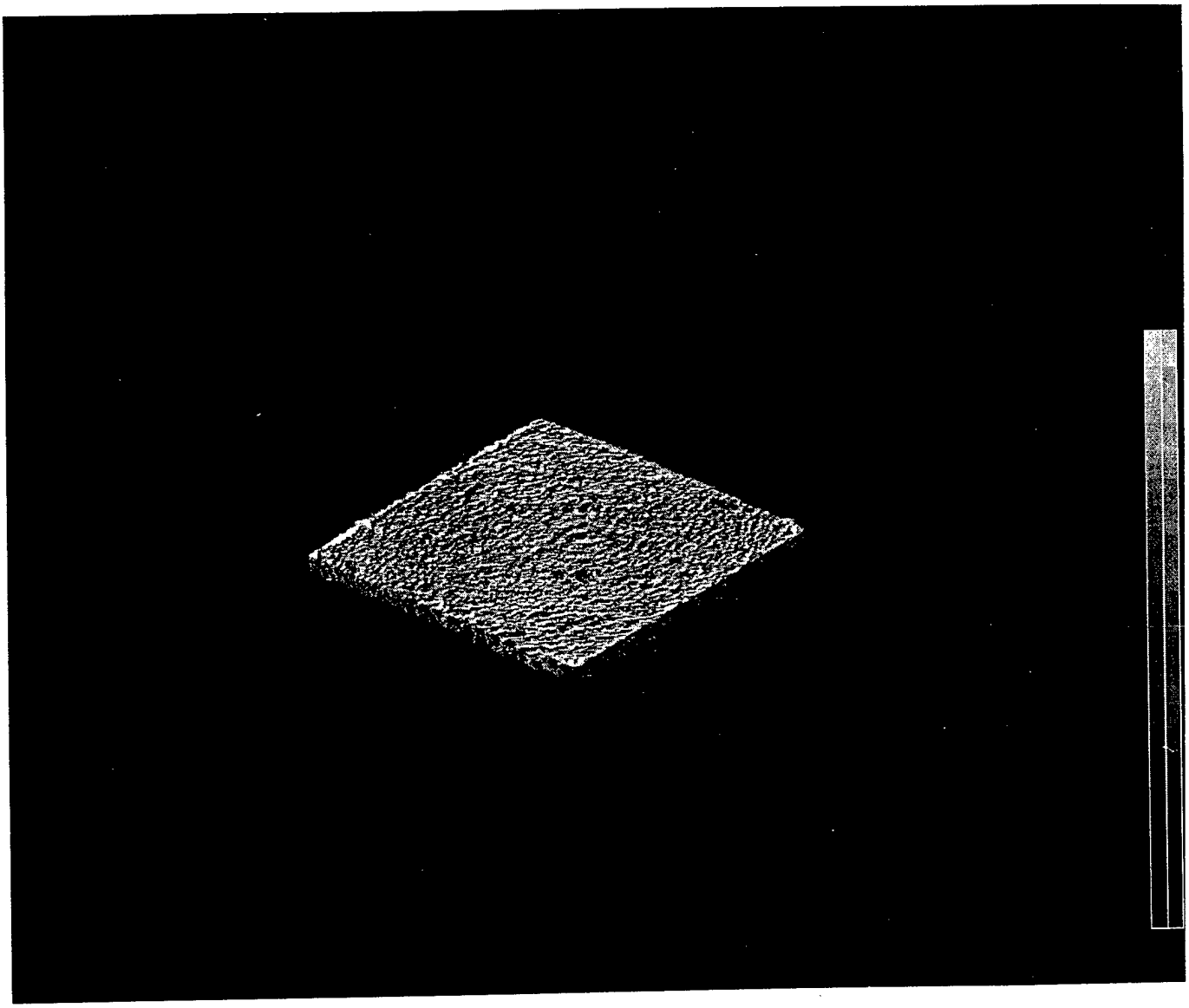

Figure 14. Volume rendering of a portion of the MPR used to get Fig. 13

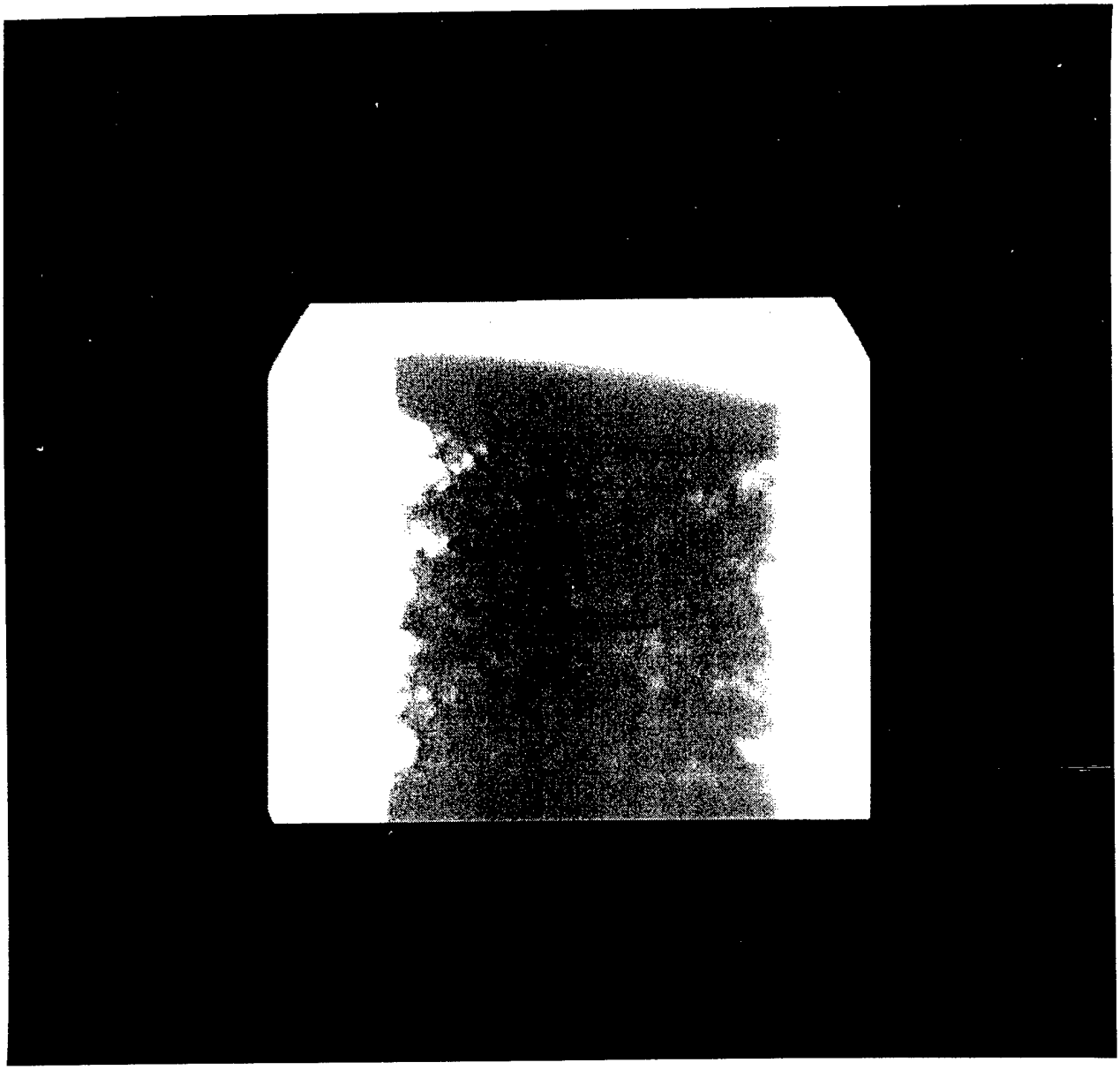

Figure 15. Digital radiograph (DR) of a cylinder excised from a foamed steel panel make using a variation of the LDC process

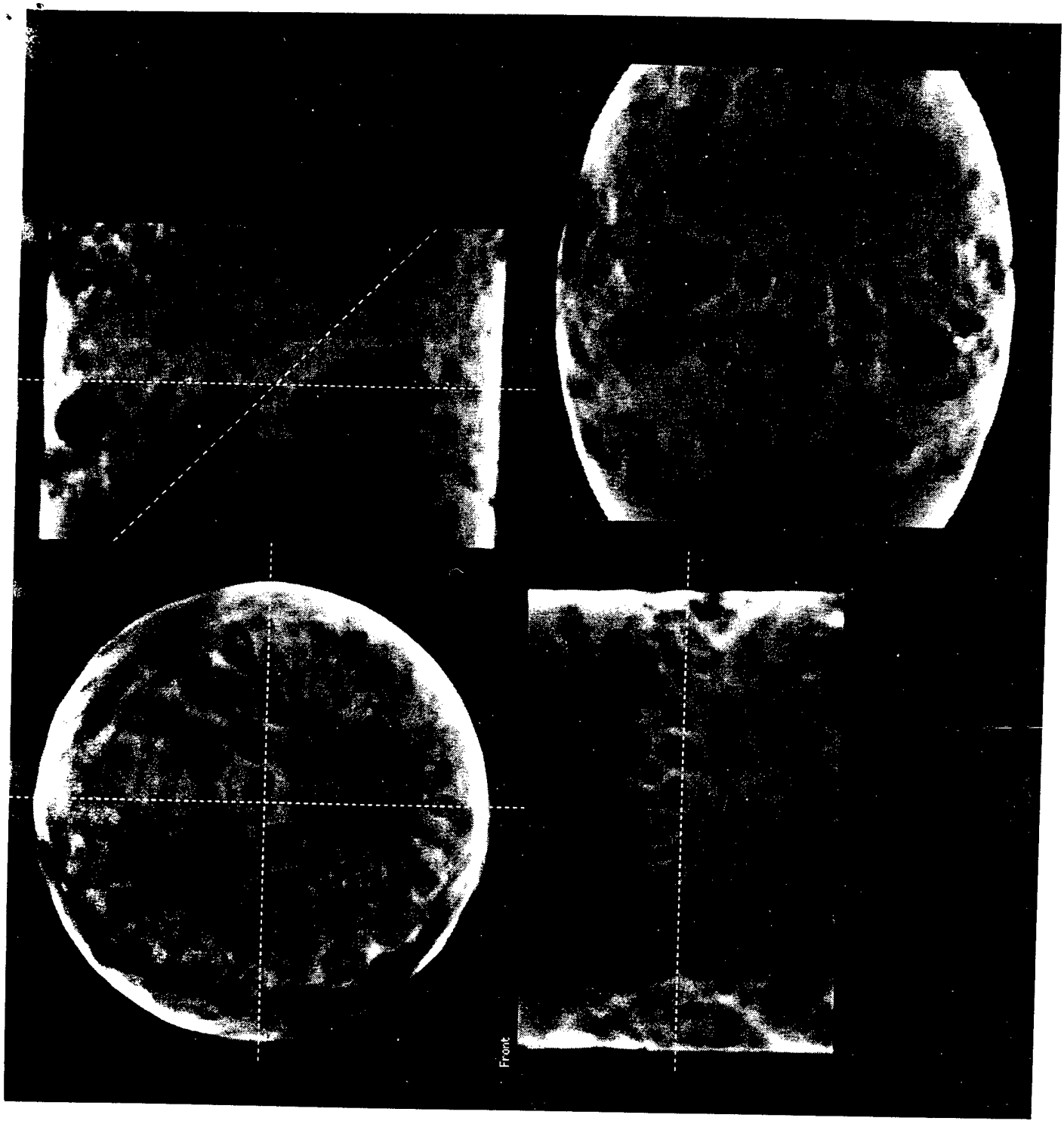

Figure 16. Same LDC foamed steel specimen as in Fig. 15. The circular image is a CT slice about half way up the cylindrical specimen, the rectangular images are vertical planes orthogonal to two diameters of the cylinder, where the diameters are perpendicular to each other

Summary

Ultralightweight metallic materials are an emerging technology with potential in a wide variety of applications ranging from commercial construction to aerospace. The various processing technologies are at different levels of development, but none have yet reached maturity. Nondestructive evaluation techniques such as computed tomography provide a promising tool for the process engineer to provide detailed feedback on the effect of process variables. Additionally, computed tomography provides specific structural information to support the effort to develop computer models for predicting the mechanical behavior of such products in various applications. This report has presented a brief tutorial on the methods of x-ray computed tomography and then given an overview of representative images which can be acquired for products from several of the varied and different processes for creating ultralightweight metallic materials.

References

1. D. S. Schwartz, D. S. Shih, A. G. Evans, and H. N. G. Wadley, eds *Porous and Cellular Materials for Structural Applications*, pp 121-132, Materials Research Society, Warrendale, PA, (1998)

2. A. C. Kak and M. Slaney, *Principles of Computerized Tomographic Imaging*, IEEE Press, N.Y., 1988.

3. J. L. Ackerman and W. A. Ellingson, eds., *Advanced Tomographic Imaging Methods for the Analysis of Materials*, Symposium held November 28-30, 1990, Boston, MA, Materials Research Society, Pittsburgh, PA., 1991.

4. D. S. Schwartz, D. S. Shih, A. G. Evans, and H. N. G. Wadley, eds *Porous and Cellular Materials for Structural Applications*, Materials Research Society, Warrendale, PA, 1998, pp. 281-290.

5. D. S. Schwartz, D. S. Shih, A. G. Evans, and H. N. G. Wadley, eds *Porous and Cellular Materials for Structural Applications*, Materials Research Society, Warrendale, PA, 1998, pp. 191-203.

6. D. S. Schwartz, D. S. Shih, A. G. Evans, and H. N. G. Wadley, eds *Porous and Cellular Materials for Structural Applications*, Materials Research Society, Warrendale, PA, 1998, pp. 133-137.

7. C-J Yu, private communication, Fraunhofer USA Resource Center, Newark, Delaware, (November, 1998)

APPENDIX I

INFORMATION EXCHANGE WITH THE COMMUNITY OF OTHER ULTRALIGHTWEIGHT METALS INVESTIGATORS

We attended the special symposium entitled "Porous and Cellular Materials for Structural Applications" at the MRS Spring Meeting in San Francisco, April 13-17, 1998 which produced Volume 521 of the MRS Symposium Proceedings Series. We learned much about the various process methods and their problems, and we were able to talk with many of the other investigators.

We participated in the meeting entitled "Ultralight Metals Study Program" at the Ocean Edge Conference Center, Brewster, MA, held August 31-September 4, 1998. The workshop was organized by Anthony Evans (then at Harvard) and Haydn Wadley (U. Virginia), as a service of their MURI on ultralight metals. We presented a paper at that meeting entitled "Nondestructive Evaluation of Ultralight Metals" in which we showed and discussed a variety of computed topographs of several ultralightweight metal specimens produced by different processes.

We participated in the Ultralight Metals Study Program in Williamsburg, VA, August 30h to September 1st, 1999. The workshop again was organized by Anthony Evans (now at Princeton) and Haydn Wadley (U. Virginia), as a service of their MURI on ultralight metals. The thrust of the program was to address new directions and applications. We presented a poster showing a variety of computed tomograpic imagery done since last year's workshop, using several more ultralight samples supplied by various processors. One of these specimens was an example of a "steel" foam produced by a process still only in early development. Another set of images were of significant interest because they showed a capability for resolving features down to nearly one thousandth of an inch (30 microns) inside a one inch specimen. Another particularly peculiar internal structure was exhibited by a 6061 aluminum specimen made by foaming compacted powders in a closed die.

At the invitation of the Fraunhofer Research Center USA in Newark, DE, we held several discussions with their management and engineers concerning how the current CT capabilities could address their most critical process control problems. As a consequence of these discussions, direct observation in real time of the progression of bubble growth during the foaming process used by Fraunhofer has been identified as a critical requirement for achieving a major improvement in their process. This information is essential to evolving a process variation producing a tighter pore size distribution. The only way to achieve this direct observation appears to be by computed tomographic imaging. We have discussed design criteria for providing a capability of processing a foam specimen in real time at a relatively high temperature within the confines of the computed tomography x-ray equipment and within the constraints of the data acquisition rates of the

system. Unfortunately, this project is unlikely to proceed, as the Director of the Fraunhofer lab in Newark, who inaugurated these discussions, has transferred back to Germany.

We have also written what we consider a definitive paper on the use of computed tomography for characterizing ultralightweight metals. It has been published in the refereed journal of record, Research in Nondestructive Evaluation:

"X-ray Computed Tomography of Ultralightweight Metals", John M.Winter, Jr., Robert E. Green, Jr., Amy M. Waters, and William H.Green, Res. Nondestr Evaluation, Wolfgang Sachse, ed-in-chief, 11, 199-211, Springer-Verlag, N.Y. (1999)